ECCM 2010
IV European Conference on Computational Mechanics
Palais des Congrès, Paris, France, May 16-21, 2010

A continuum damage mechanics based bone remodeling model in a finite strains framework.

M. Mengoni, JP. Ponthot

Non Linear Computational Mechanics, Aerospace and Mechanics Department, University of Liège, Belgium, {mmengoni,jp.ponthot}@ulg.ac.be

1 Introduction

In orthodontic treatments, loads are applied to the teeth through the use of braces or other apparatus in order for the teeth to move permanently in the bone sockets. This movement is achieved through a biochemical process of bone tissue adaptation to mechanical stimuli called bone remodeling. The word "bone remodeling" is here used for the process due to external mechanical events. Internal remodeling is not accounted for in this work. We consider, as a simplifying assumption, that its function is to renew the cells with no alteration of the overall bone mechanical properties. Therefore the internal remodeling is considered as being part only of the overall homeostatic equilibrium. For most types of bones, remodeling processes take place in order to adjust the amount of tissue and its topology according to long term loading conditions. Bone resorption occurs when disuse is observed. This resorption tends to decrease the amount of bone where it is of no mechanical relevance. Bone apposition occurs in overloaded conditions, in order to reinforce bone where it is mechanically usefull. The bone therefore adapts its density in such a way to achieve an homeostatic state of stress. Besides the density change, remodeling also occurs to change the bone topology, mainly in trabecular tissue for which the trabeculae tend to align along the principal stress directions. Bone remodeling therefore depends not only on the stress intensity but also on its orientation. A well documented example can be observed on the human femur. The trabecular architecture of its proximal end aligns with the principle stress trajectories of physiological loadings (see a literature review in [1] and Fig.1).

Contrary to the majority of bones, alveolar bone remodeling seems on a macroscopic level to depend mainly on the pressure state [2, 3, 4]. One can indeed observe apposition on the tension side of a tooth when loaded with an abnormal mechanical environment, such as the one obtained with orthodontics appliances, as well as resorption on the compression side. The actual biomechanical processes causing such a difference is not quite clear and uniformly accepted among biology and biochemistry literature (see discussions in [5, 6, 7]). To model these processes, several authors do not consider non linearities of the bone. Some authors focus only on the initial tooth mobility and extrapolate their results with a density update [2, 8] or another built-in remodeling law applied as a subsequent step to the mechanical integration [3, 9, 10]. Other authors focus on the periodontal ligament (PdL) non linear response [11]-[15]. Its non linearity and opposite behaviors in tension and compression lead to opposite loading conditions of the bone on each side of the tooth. The compressive side of the tooth would lead to underuse of the bone and therefore resorption while the tension side would get overuse and apposition. However, when no non-linearities are considered in the PdL, no difference in the strain energy on both side of a tooth can be observed. A pressure independent remodeling law used for the alveolar bone would therefore lead either to apposition or to resorption on all sides of the tooth.

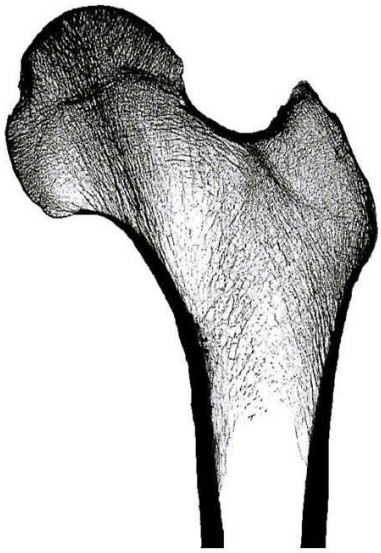

Figure 1: Human femur proximal end - trabecular architecture

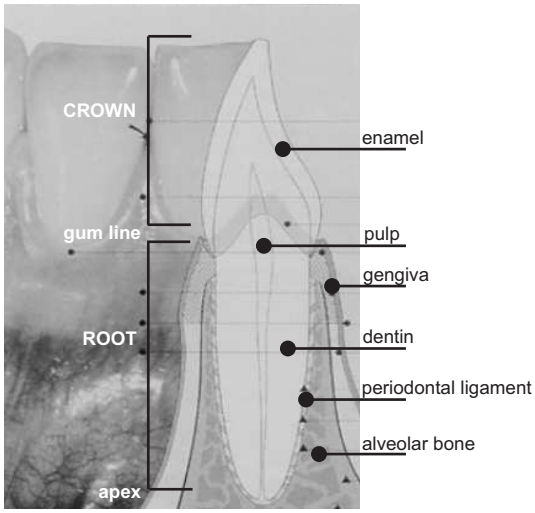

Figure 2: Tooth and surrounding tissue - anatomy (adapted from [16])

Instead of focusing on the PdL response, the present work concentrates on the bone behavior during remodeling. We assume the pressure state (positive or negative) of the bone matrix as the key stimulus to differentiate apposition and resorption in overloaded conditions. This can be justified as follows. The alveolar bone main blood and cell supply (needed for bone remodeling) is done through the periodontal ligament. As this membrane's stiffness is much less than the surrounding tissues, the strain level is high. If the hydrostatic stress level is higher than the blood vessels internal pressure, the blood flow is stopped as well as the (remodeling) cell supply to the bone. The remodeling process is therefore triggered by the PdL pressure and stopped when these stresses are too high. We therefore assume that it is the same stimulus which is responsible for the differentiation between apposition and resorption and for the triggering of the phenomenon.

2 Method.

Within the diverse approaches that have been adopted to model bone remodeling processes, most of them are qualified as phenomenological models. They are models that do not try to predict the evolution of the microstructure and biological constitution of a tissue or an organ as a consequence of the mechanical environment (contrary to mechanobiological models) but whose goal is to predict the global mechanical behavior (displacement, strains and stresses) of a tissue or an organ, taking into account the applied loads, its microstructure and the constraints imposed by other organs. Most of these models assume the existence of a given mechanical stimulus (input) that produces bone apposition or resorption (output) in such a way that the stimulus tends to a physiological level in the long-term (homeostasis). Among these phenomenological models, the definition of the mechanical stimulus uses a wide range of measures : stresses, strains, strain energy density, strain rate or even damage.

The original model which is proposed in this work is built on a previous damage/repair model. It is therefore a phenomenological model, first proposed by Doblaré and co-workers [17, 18]. This model has been chosen as a working base because it is one of the few models whose stimulus variation is justified through thermodynamical concepts of continuum mechanics. This model is first enhanced to be coupled to an elastoviscoplastic material behavior in a finite strain framework. It can therefore capture permanent strains of the tissue beyond the ones due to the density variation. The bone tissue is therefore considered as an anisotropic "organization" of elastoplastic trabeculae (although it is clear that the relevant inelastic

process is different from that of the classical metal plasticity). This "organization", as proposed in [17], is measured through a mean bone density and its anisotropy uses the concept of fabric tensor as introduced in [19]. Even tough the viscoplastic behavior may not be relevant in bone remodeling applications (due to the very low strain levels involved, permanent strains due to density variations are much higher than the one due to a plastic behavior), the proposed model can however be used both in low strain levels and higher strain levels problems keeping the continuum representation of the topology through the use of the fabric tensor and allowing to represent a viscoplastic behavior of the bone trabeculae.

Doblaré's initial model is also extended in order to be used for the particular case of the alveolar bone. The remodeling rate is therefore written to account for the pressure state of the alveolar bone so that repair will occur in the case of tissue formation, for overloaded tension conditions and damage will increase in the case of tissue resorption, both in the case of overloaded compression conditions and underloaded conditions.

We thus propose an anisotropic damage/repair model within the framework of the strain equivalence approach in continuum damage mechanics [20]. An equivalent stress tensor is defined from an objective stress tensor and two damage variables, a tensor damage measure and a scalar value measuring the importance of the hydrostatic stresses in the equivalent stress definition. The damage measure evolves in order to achieve an homeostatic level of a given stimuli. This formulation is integrated in a finite element code (home made code Metafor [21]). The main originalities with respect to [17] are therefore, first,a finite strain framework within which the model is written, allowing for the use of a elasto-plastic model for the bone matrix and, second, an extension for alveolar bone pressure dependency of the remodeling rate.

We first propose to place Doblaré's model [17, 18] in its context in order to understand all its implications.

Based on previous works, Beaupré, Carter and co-workers [22, 23] developed a model (refered here as the isotropic Stanford model) considering that bone tissue needs a certain level of mechanical stimulus to maintain homeostasis and self-regulates to maintain such a level. Their objective is to homogenize the value of a local mechanical stimulus (ψ_t, a daily stress stimulus at tissue level) in the neighborhood of an homeostatic value at tissue level, $\psi_t^\star$. This stimulus (equation 1) takes into consideration different types of loads ($i = 1 \cdots N$) as well as the number of cycles for each type of loads [n_i].

$$\psi_t = \left(\sum_{i=1}^{N} n_i \bar{\sigma}_{t_i}^m \right)^{1/m} \tag{1}$$

In equation (1), $\bar{\sigma}_t$ is a scalar measure of the stress intensity at tissue level and the m exponent is weighing the impact of stress relative to the number of load cycles. The out of equilibrium amplitude of this stimulus (the tissue level mechanical stimulus error $e_r = \psi_t - \psi_t^\star$) is considered to be the driving force for bone remodeling. A simple piecewise linear relation between the surface remodeling rate, $\dot{r}$, and this tissue level stimulus error is therefore proposed in [22] :

$$\dot{r}\,(e_r) = \begin{cases} c(e_r - \omega) & \text{for } e_r > \omega, \\ 0 & \text{for } -\omega \leq e_r \leq \omega, \\ c(e_r + \omega) & \text{for } e_r < -\omega, \end{cases} \tag{2}$$

In equation (2), c is a constant, which does not have to be equal for both cases, ω is the half-width of the so-called "dead" or lazy zone (an interval around the homeostatic level for which no remodeling processes takes place). In order to use this equation into a finite element code, distinction between tissue level and macroscopic level[1] has to be made. To distinguish between values on tissue and continuum level, the subscript t denotes tissue level. Obviously, stress defined for a continuum cannot be the same as it really appears in the microstructure. Since marrow and blood vessels filling the pores are much

[1]The macroscopic level averages the tissue density and its topology in a continuum measure.

weaker than the calcified bone tissue, the stress the tissue has to withstand will be actually greater than the continuum stress. The relation between the tissue stress measure and the continuum stress measure is given as in [24] from experimental considerations by

$$\bar{\sigma} = \left(\frac{\rho}{\rho_0}\right)^2 \bar{\sigma}_t \tag{3}$$

where ρ_0 is the density of the fully calcified bone. In [22, 23], the continuum stress measure is computed from the strain energy density in small strains elasticity:

$$\bar{\sigma} = \sqrt{E\boldsymbol{\sigma} : \varepsilon} \tag{4}$$

where ε is the Cauchy strain tensor, $\boldsymbol{\sigma}$ is the Cauchy stress tensor and E is the bone apparent Young's modulus which is dependent on the density. A commonly accepted law is

$$\begin{aligned} E &= B(\rho)\rho^{\beta(\rho)} \\ \nu &= \nu(\rho) \end{aligned} \tag{5}$$

As a particular case of equation (5), [22] chose:

$$E = \begin{cases} 2014\ \rho^{2.5}\ [MPa] & : \text{ if } \rho \leq 1.2\ g/cc \\ 1763\ \rho^{3.2}\ [MPa] & : \text{ if } \rho \geq 1.2\ g/cc \end{cases} \tag{6}$$

Finally, assuming that all formed or resorbed bone is fully mineralized gives the following density rate law :

$$\dot{\rho} = kS_v\rho_0\ \dot{r}\ (e_r) \tag{7}$$

The terms kS_v of equation (7) take into account the available ($k \in [0,1]$) bone specific surface area (S_v internal surface area per unit volume, related to the porosity $f = 1 - \frac{\rho}{\rho_0}$) as defined in [25]. An important simplification on the calculation of the daily stimulus (equation 1) can be made. As the order of loads application does not significantly affect the computational results and as the stresses can be grouped together, the daily stimulus definition simplifies as

$$\psi_t = n^{1/m}\bar{\sigma}_t \tag{8}$$

The tissue level mechanical stimulus error can be reformulated using equations (5), (3) and (8) as

$$e_r = n^{1/m}\rho_0^2\sqrt{B}\frac{\sqrt{\boldsymbol{\sigma} : \varepsilon}}{\rho^{2-\beta/2}} - \psi_t^\star \tag{9}$$

Equation (2) together with equations (7) and (9) produce an method to update the density according to the strain energy.

Jacobs and co-workers [24] present an energy based anisotropic model for bone remodeling. His assumption is that bone remodeling is an optimal process in some energetic sense. The velocity field used in the conservative laws of continuum mechanics, with the main hypothesis of small strains, therefore includes both the elastic deformation and the adaptive response. The remodeling process can be expressed as a deviation of a given stimulus from a reference one and its mathematical expression can be written as

$$f^k(\varepsilon, \mathbb{C}, \rho) \leq 0 \tag{10}$$

where the superscript k stands either for f if formation is achieved or r if resorption takes place. Assuming that bone remodeling is an optimization process gives :

$$\dot{\mathbb{C}} = \frac{\beta\,\dot{\rho}}{\rho}\frac{\boldsymbol{\sigma} \otimes \boldsymbol{\sigma}}{\boldsymbol{\sigma} : \varepsilon} \tag{11}$$

Finally, the remodeling rate is given by

$$\overset{\bullet}{r}(e_r) = \begin{cases} c\dfrac{f^f(\varepsilon,\mathbb{C},\rho)}{\rho^{2-\beta/2}} & \text{for } f^f \geq 0, f^r < 0, \\ 0 & \text{for } f^f < 0, f^r < 0, \\ -c\dfrac{f^r(\varepsilon,\mathbb{C},\rho)}{\rho^{2-\beta/2}} & \text{for } f^r \geq 0, f^f < 0, \end{cases} \tag{12}$$

This constitutive anisotropic relation reduces to the previous isotropic formulation when bone is permanently loaded by a hydrostatic stress state. The density variation can be computed from equation (7).

However, Jacobs'approach is closely related (and in fact inspired as the authors claim in [24]) to the principles of Continuum Damage Mechanics (CDM), which proposes the modification of the elastic properties according to the value of a given internal variable (the damage parameter d) related to the effective density of cracks or cavities at each point (for the isotropic case) or at each point and each direction (anisotropic case), that is, to the current microstructure [20]. The CDM theory is a phenomenological description of damage. The damage parameter is usually normalized in such a way that the value $d = 0$ corresponds to the undamaged material, while $d = 1$ represents the local rupture state or local failure of the mechanical component. CDM uses the concept of effective stress, the stress acting on the actual surface area resisting the applied force. For isotropic damage, the effective stress, $\tilde{\boldsymbol{\sigma}}$, can be written as

$$\tilde{\boldsymbol{\sigma}} = \frac{\boldsymbol{\sigma}}{1-d} \tag{13}$$

As underlined by Doblaré, Garcia and co-workers [17, 18], the anisotropic Stanford's model presents several drawbacks when compared to the generalized CDM. First of all, the stimulus is defined as a global optimization function and not, as usual in the standard theory, as a local variable. Also, the damage variable is not defined explicitly and the two internal variables (ρ and $\mathbb{C}$) are not independent. They are coupled as can be seen in equation (11), where it is shown that the evolution of the stiffness tensor depends directly on the density rate of change. To solve these difficulties, they propose a remodeling model that, after identifying the internal variables associated to the bone microstructure, follows the steps of the extension of the CDM for the anisotropic case.

In the case of bone remodeling, "damage" has to be understood as a measure of the void volume fraction inside the bone tissue, while directionality follows the idea suggested by Cowin [19] for the fabric tensor, $\hat{\boldsymbol{H}}$. The measure of damage used is therefore virtual and actually reflects the bone density that can evolve. There is no actual damage in the tissue. The undamaged material is the ideal situation of bone with null porosity and perfect isotropy. The process of bone resorption corresponds to the classical damage evolution concept, since it increases the void fraction (porosity) and therefore damage (decreases the density). However, bone apposition can reduce damage and lead to bone repair, which has to be adequately considered in this extended damage theory. As stated earlier, damage repair can be considered because the total energy dissipation includes biological dissipation due to metabolism on top of the mechanical dissipation which is negative for damage repair. Doblaré and co-workers in [17, 18] therefore define a damage tensor $\boldsymbol{D}$, related both to the density and the fabric tensor $\hat{\boldsymbol{H}}$. Using a normalization condition for $\hat{\boldsymbol{H}}$ yields to the independence of the two internal variables $\boldsymbol{D}$ and ρ and therefore solves the issue of using coupled internal variables as in Jacob's model. In analogy to plasticity, they identify an external mechanical stimulus with the variable thermodynamically associated with a remodeling tensor $\boldsymbol{H}$ function of the damage tensor $\boldsymbol{D}$. The remodeling rate $\overset{\bullet}{r}$ is obtained from the remodeling criterion (g^f in formation and g^r in resorption) that is currently active

$$\overset{\bullet}{r} = \begin{cases} c_f\dfrac{g^f}{\rho^{2-5\beta/8}} & \text{for } g^f \geq 0, g^r < 0, \\ 0 & \text{for } g^f < 0, g^r < 0, \\ -c_r\dfrac{g^r}{\rho^{2-5\beta/8}} & \text{for } g^r \geq 0, g^f < 0, \end{cases} \tag{14}$$

The density and fabric tensor evolutions are computed from the damage evolution, function of this remodeling rate.

Doblaré and co-workers [17, 18] propose an anisotropic CDM model, limited to a bone matrix described in a small strains elasticity framework, characterized by its ability to reproduce the known experimental features of bone remodeling and using independent internal variables associated to the bone microstructure. To enhance this model to a bone matrix described with a material model other than small strains linear elasticity, the effective stress definition in the representation of damage has to be chosen to enable a coupling of damage with non linearities such as viscosity or plasticity. The main drawback of Doblaré and Garcia's model for coupling with plasticity is the use of a strain energy equivalence approach to represent the contribution of damage. This approach relates the stress level in the damaged material with the stress in the undamaged material that leads to the same strain energy. This is simply done by defining an equivalent strain tensor which can be written, for isotropic damage, as

$$\tilde{\varepsilon} = (1-d)\varepsilon$$

giving the same strain energy for both the damaged and undamaged configuration.

However, this strain energy equivalence approach looses the physical relation of damage to the surface density of defects. Keeping this physical definition however, allows the coupling of damage to (visco-) plasticity by expressing the plastic criterion in terms of effective stresses instead of stresses. This strain equivalence approach gives, in small strains elasticity,[2] :

$$\tilde{\boldsymbol{\sigma}} = \mathbb{C}^o : \varepsilon \tag{15}$$

where $\mathbb{C}^o$ is Hooke's fourth order elasticity tensor for the undamaged material. This equation can also be written :

$$\boldsymbol{\sigma} = \mathbb{C} : \varepsilon \tag{16}$$

where $\mathbb{C} = (1-d)\mathbb{C}^o$ is Hooke's fourth order elasticity tensor for the damaged material. Therefore, the stiffness variation due to damage variation can be computed, similarly to equation (11), as

$$\overset{\bullet}{\mathbb{C}} = -\overset{\bullet}{d}\,\mathbb{C}^o \tag{17}$$

According to Lemaitre and Desmorat [20, 26], one of the only effective stress definition for anisotropic damage that fulfills the conditions of being symmetric, compatible with the thermodynamics (existence of a stress potential and a principle of strain equivalence) and that can express different effect on the hydrostatic and deviatoric behavior is represented by

$$\tilde{\boldsymbol{\sigma}} = \mathtt{dev}(\boldsymbol{H}\boldsymbol{s}\boldsymbol{H}) + \frac{p}{1-\frac{\eta}{3}D_{kk}}\boldsymbol{I} = \tilde{\boldsymbol{s}} + \tilde{p}\boldsymbol{I} \tag{18}$$

where $\boldsymbol{s}$ and p are respectively the stress deviator and the pressure (nominal stress $\boldsymbol{\sigma} = \boldsymbol{s} + p\boldsymbol{I}$) and where $\boldsymbol{H} = (\boldsymbol{I} - \boldsymbol{D})^{-1/2}$ is a second order symmetric tensor. This definition leads to a symmetric stress tensor and retrieves equation (13) in the case of isotropy (for which $\eta = 1$). It also leads to a locally orthotropic constitutive tensor whose principal directions of orthotropy are aligned with the principal axes of the damage tensor $\boldsymbol{D}$. In order to keep a linear relation between effective and nominal stresses as in isotropic continuum damage mechanics, one can write

$$\tilde{\boldsymbol{\sigma}} = \mathbb{M} : \boldsymbol{\sigma} \tag{19}$$

where $\mathbb{M}$ is a fourth order symmetric tensor defined from $\boldsymbol{H}$ and $D_h = \frac{1}{3}\mathtt{tr}(\boldsymbol{D})$ as

$$M_{ijkl} = H_{ik}H_{jl} - \frac{1}{3}(H_{in}H_{nj}\delta_{kl} + H_{kn}H_{nl}\delta_{ij}) + \frac{1}{9}H_{nm}H_{mn}\delta_{ij}\delta_{kl} + \frac{1}{3}\frac{1}{1-\eta D_h}\delta_{ij}\delta_{kl} \tag{20}$$

[2] While the strain energy equivalence approach would give $\tilde{\boldsymbol{\sigma}} = \mathbb{C}^o : \tilde{\varepsilon}$

Using equation (18), one can finally get

$$\left\{ \begin{array}{rcl} \tilde{p} & = & \dfrac{p}{1-\eta D_h} \\ \tilde{\boldsymbol{s}} & = & \mathbb{M} : \boldsymbol{s} \end{array} \right. \quad \text{and} \quad \left\{ \begin{array}{rcl} p & = & (1-\eta D_h)\tilde{p} \\ \boldsymbol{s} & = & \mathbb{M}^{-1} : \tilde{\boldsymbol{s}} \end{array} \right. \tag{21}$$

In order to work in a finite strain framework, we consider an additive decomposition of the strain rate tensor[3], $\boldsymbol{E}$, into its elastic and (visco-)plastic parts :

$$\boldsymbol{E} = \boldsymbol{E}^e + \boldsymbol{E}^{pl} \tag{22}$$

where $\boldsymbol{E}^{pl}$ can be calculated through the normality rule on the plastic criterion (associated plasticity) expressed in term of effective stresses. If no damage is considered, the constitutive law of the material becomes [4] :

$$\overset{\triangledown}{\boldsymbol{\sigma}} = \mathbb{C}^o : \boldsymbol{E}^e \tag{23}$$

where $\mathbb{C}^o$ is Hooke's fourth order tensor for the undamaged material, considered as constant, and $\boldsymbol{\sigma}$ is the Cauchy stress tensor[5]. For a damaged material where the strain equivalence is supposed to hold, this constitutive equation becomes :

$$\overset{\triangledown}{\tilde{\boldsymbol{\sigma}}} = \mathbb{C}^o : \boldsymbol{E}^e \tag{24}$$

The yield criterion used here for the bone is the Von Mises criterion. This assumes that only shear stresses are responsible for plastic strains. As both the triggering of bone remodeling and damage variation are function of the pressure value, this assumption may be too restrictive. However, as no data is available to us on bone behavior at plasticity, we will base our study on this restrictive hypothesis. When Von-Mises criterion is chosen, we have, only considering isotropic hardening,

$$\boldsymbol{E}^{pl} = \frac{3}{2}\frac{\dot{\lambda}}{\tilde{\sigma}_{eq}}\mathtt{dev}(\boldsymbol{H}\tilde{\boldsymbol{s}}\boldsymbol{H}) \tag{25}$$

where $\dot{\lambda}$ is the plastic multiplier and $\tilde{\sigma}_{eq}$ is the equivalent stress used for the Von-Mises criterion

$$\tilde{\sigma}_{eq} = \sqrt{\frac{3}{2}\tilde{\boldsymbol{s}} : \tilde{\boldsymbol{s}}} \tag{26}$$

Doblaré's theory can be formulated using this definition of stress as well as a strain equivalence approach. The damage tensor is therefore defined from the fabric tensor as

$$\boldsymbol{D} = \boldsymbol{I} - \left(\frac{\rho}{\rho_0}\right)^{\beta} A\hat{\boldsymbol{H}} = \boldsymbol{I} - \boldsymbol{H}^{-2} \tag{27}$$

In this damage tensor definition (equation 27), the adjusting parameter A is obtained by particularizing the anisotropic model to the isotropic case (for which the fabric tensor is a unit tensor) so that one can relate damage to the Young's modulus value. The density value is derived from the remodeling tensor, $\boldsymbol{H}$ (equation 27), when considering normalized conditions for the fabric tensor ($\det \hat{\boldsymbol{H}} = 1$).

$$\rho = \rho_0 A^{-1/\beta} \left(\det \boldsymbol{H}^{-2}\right)^{1/(3\beta)} \tag{28}$$

One can show that, in equation (28), $\det \boldsymbol{H}^{-2}$ can be computed from the damage tensor $\boldsymbol{D}$:

$$\det \boldsymbol{H}^{-2} = \det(\boldsymbol{I} - \boldsymbol{D}) = 1 - \det \boldsymbol{D} - \mathtt{tr}(\boldsymbol{D}) + \det \boldsymbol{D}\,\mathtt{tr}(\boldsymbol{D}^{-1})$$

The damage criteria is the domain of an external mechanical stimulus, $\boldsymbol{Y}$, for which damage is not modified (the lazy zone as used in the literature of bone remodeling) both for resorption and apposition.

[3] The strain rate tensor is an objective quantity.

[4] We note $\overset{\triangledown}{\boldsymbol{a}}$ an objective time derivative of $\boldsymbol{a}$ adapted to a finite strain formalism.

[5] The Cauchy stress tensor is an objective quantity.

This external mechanical stimulus, $\boldsymbol{Y}$, is identified with the variable thermodynamically associated with the remodeling tensor $\boldsymbol{H}$, choosing to use the stress as the "external driving force". We assume here that this stimulus derives only from the elastic part of the Gibbs energy, Φ.

$$\boldsymbol{Y} = \frac{\partial \Phi(\boldsymbol{\sigma}, \boldsymbol{H})}{\partial \boldsymbol{H}} \tag{29}$$

Gibbs energy is obtained, considering a linear and initially isotropic material only[6], as :

$$\Phi = \frac{1}{2}\left(\frac{1}{2G}\mathtt{tr}(\boldsymbol{H}\boldsymbol{s}\boldsymbol{H}\boldsymbol{s}) + \frac{p^2}{K(1-\eta D_h)}\right) \tag{30}$$

$\boldsymbol{Y}$ is therefore obtained in terms of the external independent variable (stress : p and $\boldsymbol{s}$) and the internal variable (remodeling tensor, $\boldsymbol{H}$) as

$$\boldsymbol{Y} = \frac{1}{2G}\boldsymbol{s}\boldsymbol{H}\boldsymbol{s} + \frac{\eta p^2}{3K(1-\eta D_h)^2}\boldsymbol{H}^{-3} \tag{31}$$

Following [17, 18] but considering a strain equivalence damage definition, we propose two damage criteria :

$$\text{Formation} : g^f = \underbrace{n^{1/m}\sqrt{B}\rho_0^{2+\beta/4}\rho^{3\beta/8}A^{-1/4}}_{U} \quad \frac{3^{1/4}}{\sqrt{1-w}}(\boldsymbol{J}:\boldsymbol{J})^{1/4} \quad -(\psi_t^\star + \omega)\rho^{2-5\beta/8} < 0 \tag{32}$$

$$\text{Resorption} : g^r = \quad -U \quad \frac{27^{1/4}}{\sqrt{1-w}}\left(\boldsymbol{J}^{-1}:\boldsymbol{J}^{-1}\right)^{-1/4} + (\psi_t^\star - \omega)\rho^{2-5\beta/8} < 0 \tag{33}$$

One can note that the resorption criterion (equation 33) is the inverse of the criterion used by [17, 18].

Considering an associated evolution law for the remodeling tensor, we can write :

$$\overset{\triangledown}{\boldsymbol{H}} = \mu^f \frac{\partial g^f}{\partial \boldsymbol{Y}} + \mu^r \frac{\partial g^r}{\partial \boldsymbol{Y}}$$

with the consistency conditions $\mu^f, \mu^r \geq 0; g^f, g^r \leq 0, \mu^f g^f = \mu^r g^r = 0$.

Deriving the remodeling criteria, combining with the remodeling tensor definition (equation 27) and the density variation of the Stanford model (equation 7), the evolution law of the remodeling tensor is written as :

$$\text{Formation} : \quad \overset{\triangledown}{\boldsymbol{H}} = -\frac{3\beta k S_v \overset{\bullet}{r}}{2\mathtt{tr}(\boldsymbol{H}^{-2}(\mathbb{W}:\boldsymbol{J})\boldsymbol{H})}\frac{\rho_0}{\rho}\mathbb{W}:\boldsymbol{J} \tag{34}$$

$$\text{Resorption} : \quad \overset{\triangledown}{\boldsymbol{H}} = -\frac{3\beta k S_v \overset{\bullet}{r}}{2\mathtt{tr}(\boldsymbol{H}^{-2}(\mathbb{W}:\boldsymbol{J}^{-3})\boldsymbol{H})}\frac{\rho_0}{\rho}\mathbb{W}:\boldsymbol{J}^{-3} \tag{35}$$

with $\boldsymbol{J} = \mathbb{W}:\boldsymbol{Y}$ and $\mathbb{W} = \frac{1}{3}(1-2w)\boldsymbol{I}\otimes\boldsymbol{I} + w\mathbf{1}$ is a fourth order pseudo-unit tensor : for $w = 1$, it is a unit deviatoric tensor, for $w = 0$, it is a unit hydrostatic tensor[7]. As two parameters, w in the definition of $\mathbb{W}$ and η in the definition of $\tilde{\boldsymbol{\sigma}}$, are defined to weigh the deviatoric and hydrostatic parts of tensors, and as they are defined on two distinct intervals ($\eta \in [1,3]$ and $w \in [0,1[$) we'll actually use $w = 0.5(\eta - 1)$ to reduce the number of parameters to one.

We thus propose an anisotropic CDM model, coupled to a bone matrix described in a finite strain elasto-(visco-)plastic framework, characterized by its ability to reproduce the known experimental features of bone remodeling and using independent internal variables associated to the bone microstructure. Even though the plastic part of the model does not play a major role in slow processes such as the ones

[6] This assumes that only the elastic part of the material behavior is relevant for the remodeling process.

[7] Let's note that for $w = 1$ however, equations (32), (34) and (35) are not defined! Therefore, $w \in [0,1[$.

inducing bone remodeling, it can be of importance in other types of processes. The proposed model can therefore be used in load situations inducing permanent strains. It gives a continuum measure of the bone architecture and density while keeping a macroscopic description of the bone tissue.

This formulation is integrated in a finite element code (in-house code Metafor [21]) using the following set of equations, whose details have been presented in this paper :

$$\begin{aligned}
\text{remodeling tensor:} \quad \boldsymbol{H} &= (\boldsymbol{I}-\boldsymbol{D})^{-1/2} \\
\text{effective stress :} \quad \tilde{\boldsymbol{\sigma}} &= \mathsf{dev}(\boldsymbol{H}\boldsymbol{s}\boldsymbol{H}) + \frac{p}{1-\frac{\eta}{3}D_{kk}}\boldsymbol{I} \\
\text{strain rate :} \quad \boldsymbol{E} &= \boldsymbol{E}^{el} + \boldsymbol{E}^{pl} \\
\text{constitutive law :} \quad \overset{\triangledown}{\tilde{\boldsymbol{\sigma}}} &= \mathbb{C}^o : (\boldsymbol{E} - \boldsymbol{E}^{pl}) \\
\text{damage variation in formation :} \quad \overset{\triangledown}{\boldsymbol{H}} &\propto -\dot{r}\,\frac{\rho_0}{\rho}\mathbb{W} : \boldsymbol{J} \\
\text{damage variation in resorption :} \quad \overset{\triangledown}{\boldsymbol{H}} &\propto -\dot{r}\,\frac{\rho_0}{\rho}\mathbb{W} : \boldsymbol{J}^{-3}
\end{aligned}$$

The time-step integration (adapted from the isotropic damage integration proposed in [27, 28]) can be described as follows : starting from a known stress state ($\boldsymbol{s}$, p) and damage ($\boldsymbol{D}$), plasticity is computed using effective stresses ($\tilde{s}$, $\tilde{p}$) with a constant damage tensor (see [29] for details on the plasticity computation), giving plastic deformations and final stresses. Damage evolution is then computed and a new value of the damage tensor is determined. Stresses and plastic deformations are then re-evaluated, up to convergence of the updated damage tensor norm. A consistent tangent operator is also proposed for this theory when integrated in this iterative process.

As stated in the introduction of this paper, this type of bone remodeling model ($\dot{r}$ as equation 14) cannot be applied to alveolar bone if no PdL nonlinearities are considered. It would indeed lead to either formation or resorption on all sides of a tooth whether the bone is submitted to tension or compression because the external mechanical stimulus does not depend on the sign of the pressure but only on its intensity ($\boldsymbol{Y} \propto p^2$). We therefore propose a model that uses an approach similar to the one exposed, for both the damage definition and variation as well as for the damage criteria. However, in accordance to the observation of a pressure dependent phenomenon, the remodeling rate definition is modified (Fig.3, equation 36) taking into account the pressure state.

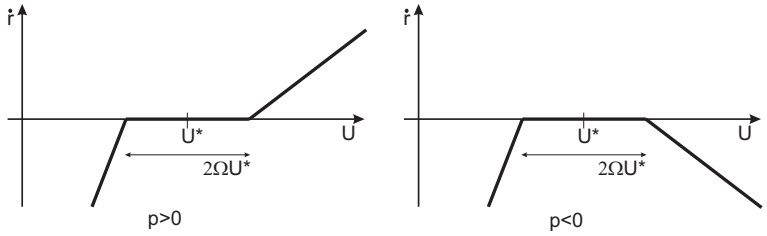

Figure 3: Pressure dependent remodeling rate, pressure p being positive in tension.

We here therefore consider an overload criterion g_o that can be expressed as the formation criterion (equation 32) and an underload criterion g_u, expressed as the resorption criterion (equation 33). This new remodeling rate is thus given by :

$$\dot{r}_p = \begin{cases} c_f \dfrac{g_o}{\rho^{2-\beta/2}} & \text{if } g_o \geq 0,\ g_u < 0 \quad \text{and} \quad p > 0 \\ -c_r \dfrac{g_u}{\rho^{2-\beta/2}} & \text{if } g_o \geq 0,\ g_u < 0 \quad \text{and} \quad p < 0 \\ 0 & \text{if } g_o < 0,\ g_u < 0 \\ -c_r \dfrac{g_u}{\rho^{2-\beta/2}} & \text{if } g_u \geq 0,\ g_o < 0 \end{cases} \tag{36}$$

where c_r and c_f are two remodeling constants, β is the density related parameter introduced in equation (5) and p, the pressure is positive in tension. For numerical purposes, the differentiation between formation and resorption when $g_o \geq 0$ is not exactly at $p = 0$ but at $p = \pm\delta p \ll 1$. A linear regression for the remodeling coefficient between $p = -\delta p$ (use of c_r) and $p = \delta p$ (use of c_f) is used. The damage evolution is proportional to the defined remodeling rate so that repair will occur in the case of tissue formation, for overloaded tension conditions. Damage will increase in the case of tissue resorption, both in the case of overloaded compression conditions and underloaded conditions. Therefore, when underloaded, the alveolar bone would resorb, as it is observed following the loss of a tooth. However, when overloaded, such as when following orthodontic treatment, the bone will resorb where it is compressed and will be formed where it is in tension so that the tooth will move in its socket along the direction of the applied force.

3 Results

This bone remodeling model is first used on the alveolar bone surrounding a 2D model of a tooth. The aim is to predict the bone density and its evolution from an initial ideal situation (isotropic material with uniform density distribution) when loaded by forces that characterize orthodontic appliances such as brackets. The tooth's movement represented is a tipping movement in the vestibulo-lingual direction, achieved either by imposed rotation of a rigid tooth or by imposed pressure on an elastic tooth's crown. The geometry of the tooth is idealized, with a parabolic root surrounded by a constant thickness periodontal ligament as well as trabecular and cortical bone. The 2D geometry and discretization used here are shown in Fig.4 and have been described in [28]. The tooth and the PdL mechanical behavior are considered as linear elastic ($E_{\text{tooth}} \approx 20GPa$, $\nu_{\text{tooth}} = 0.3$, $E_{\text{PdL}} = 0.6MPa$, $\nu_{\text{PdL}} = 0.49$ - quasi-incompressible). The cortical layer as well as the trabecular bone mechanical behavior is elasto-plastic with the anisotropic continuum damage model described in this paper to represent bone remodeling.

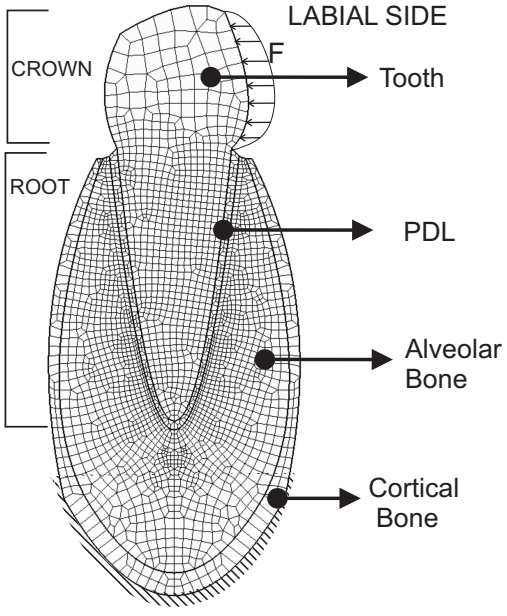

Figure 4: 2D mesh and boundary conditions of the tooth and its surrounding tissues.

Finite Element analysis is performed, using finite strains code Metafor [21], considering a plane strain state as well as a quasi-static analysis. The basal bone junction is fixed in both vertical and horizontal directions. The initial situation corresponds for the alveolar bone to an isotropic homogeneous state with initial density $\rho = 1.0g/cc$ (this density value corresponds to a porosity of .5 and a damage of .88). We

used the following set of parameters :

- $\psi^\star = 10\ MPa/day$ (homeostatic value of the stimulus)
- $N = 10^3$ (number of load cycles a day)
- $m = 4$ (exponent of the stress stimulus, ψ_t)
- $c_r = c_f = 0.1 \frac{\mu m/day}{MPa/day}$ (remodeling velocity for resorption and formation)
- $\omega = 25\%\psi^\star$ (half-width of the dead zone)
- $\eta = 1.2$ (parameter weighing the hydrostatic and deviatoric parts of the effective stress definition)[8].

Results are here presented for the load case consisting of a pressure force applied at the labial side of the crown with a pressure value corresponding to a $1N$ homogeneously distributed force. The force is maintained during 3 weeks, considering a thousand cycles a day. Bone remodeling is observed around the apex of the tooth, resorption on the labial side and apposition on the lingual one. One can observe that this tooth movement induces both a change of density as well as a change of orientation in the alveolar bone structure. Fig.5 shows density values range from .6 to 1.3 gr/cc and also shows the anisotropy behavior represented by fabric surfaces - graphical representation of the fabric tensor values along each direction - at some arbitrary Gauss points. This change in fabric principal direction can be directly related to a change in the bone microstructure. The trabecular orientation where bone remodeling is observed aligns in such a way that bone fibers are perpendicular to the tooth root surface (damage is greater along the root), except at the apex where the hydrostatic state of the bone switches from compression to tension values. It can also be shown that the damage principal directions align with the stresses principal directions.

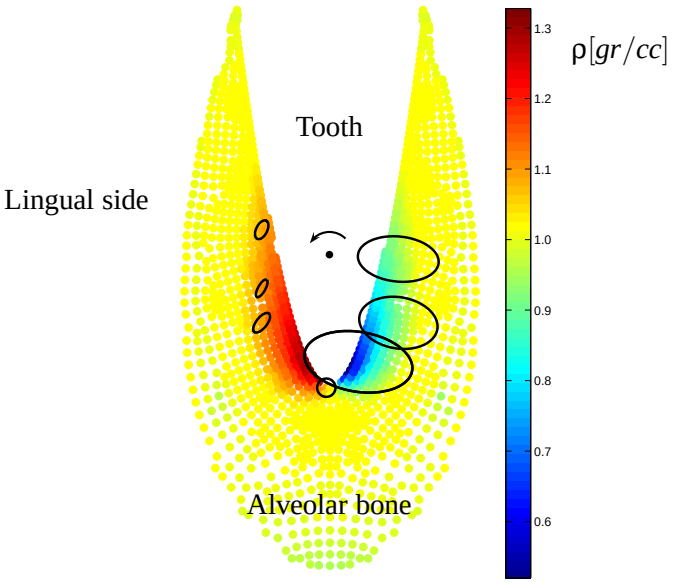

Figure 5: Alveolar Bone - Distribution of bone density a Gauss points, starting from uniform density of $1.0 g/cc$, due to a bucco-lingual rotation of the tooth (after 3 weeks of constant pressure). Ellipses show the fabric anisotropy at some arbitrary locations (their axes length are inversely proportional to Young's modulus in that direction).

[8] w is therefore equal to 0.3 as used for other type of bone remodeling issues in [17, 30]

The bone remodeling model is also used, without its extension for alveolar bone, to analyze the bone structure evolution of a 3D model of a proximal extremity of a femur. The 3D mesh is obtained from a discretized surface data available from the VAKHUM dataset [31] (consisting for the whole femur of 4232 triangular cells). The proximal end of the femur is extracted from this surface and a volume mesh is generated by the use of Tetgen [32]. The final 3D mesh consisting of 22669 linear tetrahedron and 4661 nodes is shown on Fig.6.

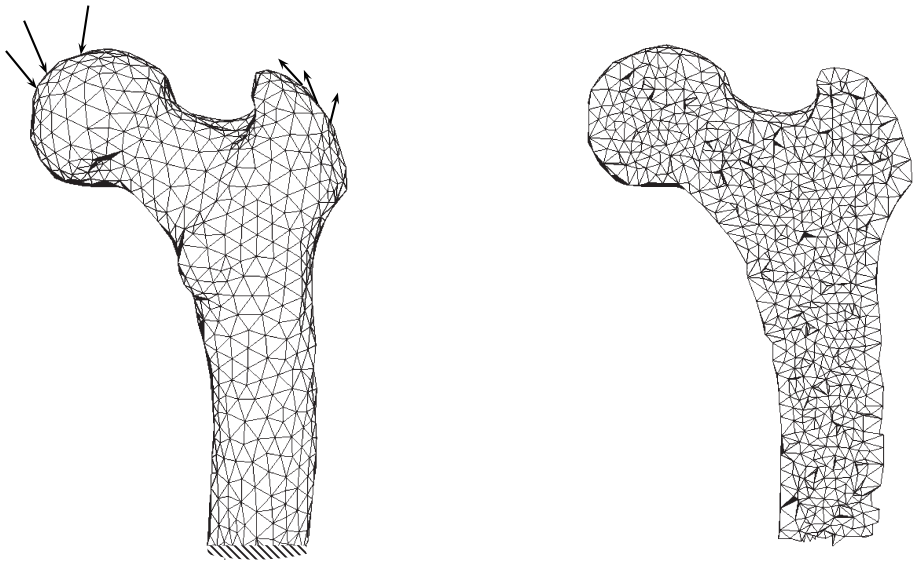

Figure 6: Left - 3D mesh and boundary conditions of the proximal extremity of the femur. Right - frontal cut through the mesh.

Following the same scheme as in [17, 30], we considered the remodeling behavior under the action of three simultaneous load cases that characterize the gait movement. The initial situation corresponds to an isotropic homogeneous state with initial density $\rho = 1.8 g/cc$ (corresponding to a porosity of .15). The following set of parameters was used :

- $\psi^\star = 50\ MPa/day$ (homeostatic value of the stimulus)
- $N = 5000$ (number of load cycles a day)
- $m = 4$ (exponent of the stress stimulus, ψ_t)
- $c_r = c_f = 0.02 \frac{\mu m/day}{MPa/day}$ (remodeling velocity for resorption and formation)
- $\omega = 25\% \psi^\star$ (half-width of the dead zone)
- $\eta = 1.2$ (parameter weighing the hydrostatic and deviatoric parts of the effective stress definition)

When comparing Fig.1, showing a section of the proximal extremity of a healthy bone for which the density distribution is related to the gray-scale of the picture, to the results of the simulation presented in Fig.7, we observe a similarity to the reality, morphologically speaking (as well as the same qualitative results as previous models [17, 24]).

4 Conclusions

The present study introduces a numerical model for the simulation of orthodontic tooth movement based on the assumption that bone remodeling processes during tooth movement are controlled by elastic en-

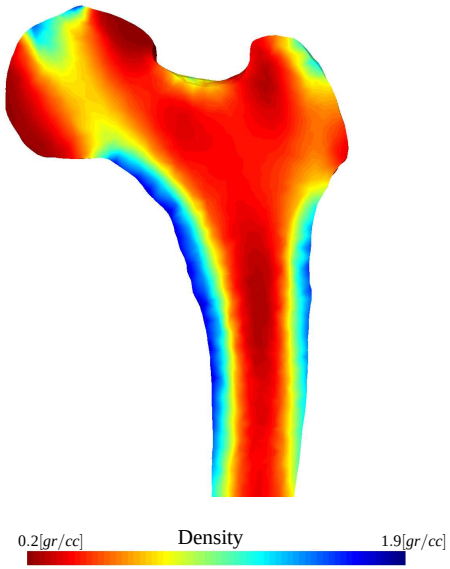

Figure 7: Proximal Femur Bone Remodeling : Distribution of densities starting from uniform density of $1.8g/cc$, 5000 gait cycles a day (10 days). The base of the femur head is considered as fixed.

ergy density as well as pressure state of the alveolar bone. The model is built on a damage-repair law proposed by Doblaré and co-workers [17]. This model has been chosen as a working framework because it is one of the few models whose stimulus variation is justified through thermodynamical concepts of continuum mechanics. It identifies the bone voids with the cavities or microcracks of other material damage models, but changes some of the standard assumptions to adapt it to the special requirements of living tissues, especially the possibility of decreasing the damage level (repair) by providing the required metabolic energy [17]. Its main drawback is the elastic character of the bone matrix which therefore does not include permanent strains of the bone matrix as a possible mechanism to get irreversible movements of a tooth in its socket.

We therefore propose an enhanced model to be used in a finite strain framework and for the specificities of alveolar bone remodeling. We assume for the bone matrix a generalized material model and considered it to be elasto-viscoplastic. The coupling of plasticity and damage is obtained using a strain equivalence approach for the effective state in a continuum damage framework. The model can therefore be used to predict long term tooth movement due both to remodeling and permanent strains of the bone matrix. The main restriction of the model is the choice made for the yield criterion. As no data is available to us on bone behavior at plasticity, we consider only a Von-Mises plasticity. This assumes that only shear stress is responsible for plastic strains. This hypothesis needs to be confronted to experimental data on bone's yield behavior in order for the model to be validated. The pressure dependency of alveolar bone remodeling is also treated, proposing a new remodeling rate formulation.

The bone model is successfully applied to different types of bones and loadings. We present some results on the remodeling obtained around a tooth when a tipping movement is reached in an orthodontic treatment. The model predicts variation of density as well as alveolar bone orientation obtained with this tooth movement that seems coherent with the observation. We also successfully used the remodeling model to analyze the structure evolution of a $3D$ proximal femur under the action of loads representative of gait movement.

References

[1] J. G. Skedros and S. L. Baucom. Mathematical analysis of trabecular [']trajectories' in apparent trajectorial structures: The unfortunate historical emphasis on the human proximal femur. *Journal of Theoretical Biology*, 244(1):15 – 45, 2007.

[2] B. Melsen. Tissue reaction to orthodontic tooth movement–a new paradigm. *Eur. J. Orthod.*, 23(6):671–681, Dec 2001.

[3] C. Bourauel, D. Freudenreich, D. Vollmer, D. Kobe, D. Drescher, and A. Jäger. Simulation of orthodontic tooth movements. a comparison of numerical models. *J. Orofac. Orthop.*, 60(2):136–151, 1999.

[4] C. Bourauel, D. Vollmer, and A. Jäger. Application of bone remodeling theories in the simulation of orthodontic tooth movements. *J. Orofac. Orthop.*, 61(4):266–279, 2000.

[5] W. E. Roberts, S. Huja, and J. A. Roberts. Bone modeling: biomechanics, molecular mechanisms, and clinical perspectives. Seminars in Orthodontics, 2004. Volume 10, Issue 2, June 2004, Pages 123-161.

[6] V. Krishnan and Z. Davidovitch. Cellular, molecular, and tissue-level reactions to orthodontic force. *Am. J. Orthod. Dentofacial Orthop.*, 129(4):469.e1–469.32, Apr 2006.

[7] R. S. Masella and M. Meister. Current concepts in the biology of orthodontic tooth movement. *Am. J. Orthod. Dentofacial Orthop.*, 129(4):458–468, Apr 2006.

[8] P. M. Cattaneo, M. Dalstra, and B. Melsen. The finite element method : a tool to study orthodontic tooth movement. *J. Dent. Res.*, 84(5):428–433, 2005.

[9] Y. Kojima, T. Mizuno, and H. Fukui. A numerical simulation of tooth movement produced by molar uprighting spring. *Am. J. Orthod. Dentofacial Orthop.*, 132:630–638, 2007.

[10] J. Schneider, M. Geiger, and F.-G. Sander. Numerical experiments on long-time orthodontic tooth movement. *Am. J. Orthod. Dentofacial Orthop.*, 121(3):257–265, Mar 2002.

[11] A. Natali, editor. *Dental Biomechanics*. Taylor and Francis, 2003.

[12] A. N. Natali, E. L. Carniel, P. G. Pavan, C. Bourauel, A. Ziegler, and L. Keilig. Experimental-numerical analysis of minipig's multi-rooted teeth. *J. Biomech.*, 40(8):1701–1708, 2007.

[13] C. G. Provatidis. A comparative fem-study of tooth mobility using isotropic and anisotropic models of the periodontal ligament. finite element method. *Med. Eng. Phys.*, 22(5):359–370, Jun 2000.

[14] S.R. Toms and Eberhardt A.W. A nonlinear finite element analysis of the periodontal ligament under orthodontic tooth loading. *Am. J. Orthod. Dentofacial Orthop.*, 123(6):657–665, Jun 2003.

[15] C. Verna, M. Dalstra, T. Clive Lee, P. M. Cattaneo, and B. Melsen. Microcracks in the alveolar bone following orthodontic tooth movement: a morphological and morphometric study. *Eur. J. Orthod.*, 26(5):459–467, Oct 2004.

[16] A. Vanheudsen. *Anatomie de l'appareil masticateur, cours de 2eme bachelier sciences dentaires*. University of Liège, 2008.

[17] M. Doblaré and J. M. García. Anisotropic bone remodelling model based on a continuum damage-repair theory. *J. Biomech.*, 35(1):1–17, Jan 2002.

[18] J. M. García, M. Doblaré, and J. Cegonino. Bone remodelling simulation: a tool for implant design. *Computational Materials Science*, 25(1-2):100–114, September 2002.

[19] S. C. Cowin, R. T. Hart, J. R. Balser, and D. H. Kohn. Functional adaptation in long bones: establishing in vivo values for surface remodeling rate coefficients. *J. Biomech.*, 18(9):665–684, 1985.

[20] J. Lemaitre and R. Desmorat. *Engineering Damage Mechanics: Ductile, Creep, Fatigue and Brittle Failures*. Springer, 2005.

[21] Metafor. *A large strain finite element code*. LTAS - MN2L / University of Liège, http://metafor.ltas.ulg.ac.be/ , 2009.

[22] G. S. Beaupré, T. E. Orr, and D. R. Carter. An approach for time-dependent bone modeling and remodeling–theoretical development. *J. Orthop. Res.*, 8(5):651–661, Sep 1990.

[23] G. S. Beaupré, T. E. Orr, and D. R. Carter. An approach for time-dependent bone modeling and remodeling-application: a preliminary remodeling simulation. *J. Orthop. Res.*, 8(5):662–670, Sep 1990.

[24] C. R. Jacobs, J. C. Simo, G. S. Beaupre, and D. R. Carter. Adaptive bone remodeling incorporating simultaneous density and anisotropy considerations. *J. Biomech.*, 30(6):603–613, June 1997.

[25] R.B. Martin. Porosity and specific surface of bone. *Crit. Rev. Biomed. Eng.*, 10(3):179–222, 1984.

[26] R. Desmorat and S. Otin. Cross-identification isotropic/anisotropic damage and application to anisothermal structural failure. *Engineering Fracture Mechanics*, 75:3446–3463, 2008.

[27] P.P. Jeunechamps. *Simulation numérique, à l'aide d'algorithmes thermomécaniques implicites, de matériaux endommageables pouvant subir de grandes vitesses de déformation. Application aux structures aéronautiques soumises à impact.* Phd thesis (in french), University of Liège (Belgium), School of Engineering, Aerospace and Mechanics Department, 2008.

[28] M. Mengoni and J.P. Ponthot. Isotropic continuum damage/repair model for alveolar bone remodeling. *Journal of Computational and Applied Mathematics*, 2009. doi:10.1016/j.cam.2009.08.061 - accepted for publication.

[29] J.P. Ponthot. Unified stress update algorithms for the numerical simulation of large deformation elasto-plastic and elasto-viscoplastic processes. *International Journal of Plasticity*, 18:91–126, 2002.

[30] M. Doblaré and J. M. García. Application of an anisotropic bone-remodelling model based on a damage-repair theory to the analysis of the proximal femur before and after total hip replacement. *Journal of Biomechanics*, 34:1157–1170, 2001.

[31] VAKHUM. *Virtual Animation of the Kinematics of the Human for Industrial, Educational and Research Purposes.* European Project (# IST-1999-10954), www.ulb.ac.be/project/vakhum/ , 2009.

[32] Hang Si. *Tetgen, a quality tetrahedral mesh generator and three-dimensional Delaunay triangulator.* http://tetgen.berlios.de, 2006.